rheumatoid arthritis. JAMA 1949;140:659-62.
9. Northrup Grumman Corporation. MedDRA and the MSSO. Northrup Grumman Corporation website [Internet. Accessed February 6, 2009.] Available from: http://www.meddramsso.com/MSSOWeb/index.htm
10. ICH Steering Committee. ICH Harmonised Tripartite Guideline. Clinical safety data management: definitions and standards for expedited reporting. Pharmaceuticals and Medical Devices Agency website [Internet. Accessed February 6, 2009.] Available from: http://www.pmda.go.jp/ich/e/e2a_95_3_20e.pdf
11. van Gestel AM, Prevoo ML, van 't Hof MA, van Rijswijk MH, van de Putte LB, van Riel PL. Development and validation of the European League Against Rheumatism response criteria for rheumatoid arthritis. Comparison with the preliminary American College of Rheumatology and the World Health Organization/International League Against Rheumatism criteria. Arthritis Rheum 1996;39:34-40.
12. Prevoo ML, van 't Hof MA, Kuper HH, van Leeuwen MA, van de Putte LB, van Riel PL. Modified disease activity scores that include twenty-eight-joint counts. Development and validation in a prospective longitudinal study of patients with rheumatoid arthritis. Arthritis Rheum 1995;38:44-8.
13. American College of Rheumatology Subcommittee on Rheumatoid Arthritis Guidelines. Guidelines for the management of rheumatoid arthritis: 2002 Update. Arthritis Rheum 2002;46:328-46.
14. Bernatsky S, Feldman D, Shrier I, et al. Care pathways in early rheumatoid arthritis. Can Fam Physician 2006;52:1444-5.
15. Donahue KE, Gartlehner G, Jonas DE, et al. Systematic review: Comparative effectiveness and harms of disease-modifying medications for rheumatoid arthritis. Ann Intern Med 2007;124-34.
16. van Riel PL, Taggart AJ, Sany J, et al. Efficacy and safety of combination etanercept and methotrexate versus etanercept alone in patients with rheumatoid arthritis with an inadequate response to methotrexate: The ADORE study. Ann Rheum Dis 2006;65:1478-83.
17. Keystone EC, Schiff MH, Kremer JM, et al. Once-weekly administration of 50 mg etanercept in patients with active rheumatoid arthritis: results of a multicenter, randomized, double-blind, placebo-controlled trial. Arthritis Rheum 2004;50:353-63.
18. Klareskog L, van der Heijde D, De Jager JP, et al. Therapeutic effect of the combination of etanercept and methotrexate compared with each treatment alone in patients with rheumatoid arthritis: double-blind randomised controlled trial. Lancet 2004;363:675-81.
19. Hamdi H, Mariette X, Godot V, et al. Inhibition of anti-tuberculosis T-lymphocyte function with tumour necrosis factor antagonists. Arthritis Res Ther 2006;8:R114.
20. Botha T, Ryffel B. Reactivation of latent tuberculosis infection in TNF-deficient mice. J Immunol 2003;171:3110-8.
21. Desai SB, Furst DE. Problems encountered during anti-tumour necrosis factor therapy. Best Pract Res Clin Rheumatol 2006;20:757-90.
22. Long R, Gardam M. Tumour necrosis factor-alpha inhibitors and the reactivation of latent tuberculosis infection. CMAJ 2003;168:1153-6.
23. World Health Organization. Global tuberculosis control: surveillance, planning, financing: WHO Report 2007. World Health Organization website. [Internet. Accessed February 6, 2009.] Available from: http://www.who.int/tb/en/
24. Bathon JM, Martin RW, Fleischmann RM, et al. A comparison of etanercept and methotrexate in patients with early rheumatoid arthritis. N Engl J Med 2000;343:1586-93.
25. Jundt JW, Browne BA, Fiocco GP, Steele AD, Mock D. A comparison of low dose methotrexate bioavailability: oral solution, oral tablet, subcutaneous and intramuscular dosing. J Rheumatol 1993;20:1845-9.
26. van der Heijde D, Da Silva JC, Dougados M, et al. Once-weekly 50-mg dosing of Etanercept (Enbrel®) is as effective as 25-mg twice-weekly dosing in patients with ankylosing spondylitis. Ann Rheum Dis 2006;65:1572-7.

International Immunology, Vol. 21, No. 6, pp. 645–654
doi:10.1093/intimm/dxp033

Dopamine released by dendritic cells polarizes T_h2 differentiation

Kazuhisa Nakano[1,2], Takehiro Higashi[1], Rie Takagi[1], Kumiko Hashimoto[1], Yoshiya Tanaka[2] and Sho Matsushita[1]

[1]Department of Allergy and Immunology, Faculty of Medicine, Saitama Medical University, 38 Morohongo, Moroyama, Saitama 350-0495, Japan
[2]First Department of Internal Medicine, School of Medicine, University of Occupational and Environmental Health, Kitakyushu 807-8555, Japan

Keywords: CD4 T cells, cell differentiation, dendritic cells, dopamine

Abstract

A major neurotransmitter dopamine transmits signals via five different seven transmembrane G protein-coupled receptors termed D1–D5. It is now evident that dopamine is released from leukocytes and acts as autocrine or paracrine immune modulator. However, the role of dopamine for dendritic cells (DCs) and T_h differentiation remains unclear. We herein demonstrate that human monocyte-derived dendritic cells (Mo-DCs) stored dopamine in the secretary vesicles. The storage of dopamine in Mo-DCs was enhanced by forskolin and dopamine D2-like receptor antagonists via increasing cyclic adenosine 3′,5′-monophosphate (cAMP) formation. Antigen-specific interaction with naive $CD4^+$ T cells induced releasing dopamine-including vesicles from Mo-DCs. In naive $CD4^+$ T cells, dopamine dose dependently increased cAMP levels via D1-like receptors and shifts T-cell differentiation to T_h2, in response to anti-CD3 plus anti-CD28 mAb. Furthermore, we demonstrated that dopamine D2-like receptor antagonists, such as sulpiride and nemonapride, induced a significant DC-mediated T_h2 differentiation, using mixed lymphocyte reaction between human Mo-DCs and allogeneic naive $CD4^+$ T cells. When dopamine release from Mo-DCs is inhibited by colchicines (a microtubule depolymerizer), T-cell differentiation shifts toward T_h1. These findings identify DCs as a new source of dopamine, which functions as a T_h2-polarizing factor in DC-naive T-cell interface.

Introduction

Dendritic cells (DCs), the most powerful antigen-presenting cell (APC) of the immune system, play a critical role in the induction of primary immune responses and immunological tolerance as well as for the regulation of T_h1 and T_h2 immune responses (1). They reside in an immature state in many non-lymphoid tissues such as the skin or airway mucosa which are under high exposure of pathogens and chemicals. Therefore, the surrounding microenvironment affects their character as professional APC.

It is well known that the ligands for many isoforms of toll-like receptors, including certain nucleic acids, LPSs and fungus-derived glycoprotein molecules, alter the DC function and induce T_h1 differentiation in an antigen non-specific manner (2). In this process, IL-12 produced by DCs is clearly correlated with sensitization of T_h1 lymphocytes *in vitro* and *in vivo* among the factors that have been shown to influence the T_h1–T_h2 balance (3).

On the other hand, DCs matured in the presence of prostaglandin E_2 (PGE_2), histamine or forskolin induce the differentiation of naive $CD4^+$ T cells toward T_h2 via the cyclic adenosine 3′,5′-monophosphate (cAMP) cascade (4–6). Several reports by others have shown the up-regulation of the CD86 surface expression of APC (7, 8) or the suppression of IL-12 production (9, 10) to be associated with an increased T_h2 response. However, which specific molecules positively induce a significant T_h2 differentiation during the interaction between DC and naive $CD4^+$ T cells still remains to be clarified and the contribution of the DC itself to T_h2 differentiation remains unclear.

It is now clear that T-cell activation requires a zone of adhesive, direct contact with APCs popularly known as the immune synapse (11). The immune synapse exhibits many similarities with classical neuronal synapses, including a requirement for cell-to-cell adhesion and close membrane

Correspondence to: S. Matsushita; E-mail: shomat@saitama-med.ac.jp

Transmitting editor: K. Okumura

Received 5 November 2008, *accepted* 4 March 2009

Advance Access publication 30 March 2009

apposition. In addition, triggering of cell surface receptors leads to intracellular signal transduction in both structures (12). Recent studies revealed that some neurotransmitters, such as serotonin (5-HT) and glutamate secreted by DCs, were released for naive T cells during DC–T-cell interaction, leading to activate T cells in mice and humans (13, 14).

Dopamine is a major monoamine neurotransmitter in the central nervous system, being involved in functions, such as movement, endocrine regulation and cardiovascular function. In the periphery, dopamine is primarily the precursor of noradrenaline and adrenaline, the major neurotransmitter of the sympathetic nerve system and the major adrenomedullary hormone, respectively. In dopamine-producing cells, the rate-limiting step in catecholamine biosynthesis is the oxidation of tyrosine to dihydroxyphenylalanine (DOPA) by tyrosine hydroxylase (TH). Next, DOPA is decarboxylated to dopamine by aromatic L-amino acid decarboxylase and stored in vesicles. TH is activated by an increased level of cAMP (15).

Five types of dopamine receptors termed D1–D5 have been identified to date (16). They belong to the family of seven transmembrane G protein-coupled receptors (GPCRs) and they have been classified into two subgroups, based on the genomic structure and pharmacological properties. D1 and D5 form the D1-like group that couples with the Gαs class of G proteins, leading to an increase in intracellular cAMP formation, while D2, D3 and D4 form the D2-like group that couples with the Gαi class of G proteins, leading to a decrease in intracellular cAMP formation (16).

Until a few years ago, dopamine was considered mainly as a conventional neurotransmitter and a neuroendocrine mediator; however, the influence of dopamine on immune cells has received much attention because of the presence of dopamine receptors on T cells. In both *in vitro* and *in vivo* studies, dopamine has been shown to either inhibit the proliferation and production of cytokines or induce the apoptosis of lymphocytes, therefore indicating an immunosuppressive activity (17, 18). Although the presence of catecholamine synthetic pathway in lymphocytes has been already described in 1994 (19), recent reports showed that regulatory T (Treg) cells (20) and polymorphonuclear cells (21), such as macrophages and neutrophils, are also capable of *de novo* production of catecholamines. These evidences contribute to understand the cross-talk between the immune and nervous systems.

Because schizophrenia is associated with excessive stimulation of D2-like receptors by dopamine (22), the D2-like antagonist is the most widely used treatment for schizophrenia. In schizophrenic patients, it has been reported that the expression of D2-like receptors increased not only in the brain (23) but also in the immune cells (24, 25) when compared with non-schizophrenic patients. This finding suggests that D2-like antagonists may modulate cytokine balances via D2-like receptors on immune cells. Indeed, several studies have assessed serum or plasma levels of both IFN-γ and IL-4 (26, 27). It is noteworthy that IFN-γ–IL-4 levels in plasma are significantly higher in medication-naive (first onset) or medication-free schizophrenic patients than in healthy controls and that the increased levels of IFN-γ–IL-4 attenuated by effective neuroleptic treatment (26). We herein hypothesized that DCs, which are ubiquitously distributed in peripheral tissues where they serve as immune sensors, are one of the major sources of dopamine and that dopamine is released upon interaction with naive $CD4^+$ T cells, thereby regulating T_h1–T_h2 polarization.

In the present study, we demonstrated that human monocyte-derived dendritic cells (Mo-DCs) stored dopamine and that dopamine was released upon interaction with naive $CD4^+$ T cells, thereby polarizing T_h2 differentiation via cAMP formation in naive $CD4^+$ T cells.

Methods

Preparation of human Mo-DCs and T lymphocytes

Human Mo-DCs and $CD45RA^+$ naive T cells (>99% purity) were prepared as previously described (28). The study using peripheral blood of healthy volunteers was approved by Saitama Medical University Ethics Committee.

Immunofluorescent detection of dopamine

Immature Mo-DCs, stimulated with 10 μM forskolin (Sigma), 0.1 μM sulpiride (a selective D2-like receptor antagonist) or 10^{-7} M α-methyl-*para*-tyrosine (a TH inhibitor) for 48 h, were collected, prefixed with 50 mM cacodylate and 1% sodium metabisulfite (MBS) and fixed with 5% glutaraldehyde (GA) in 0.1 M cacodylate and 1% MBS for 15 min. After washing with 1% MBS in 50 mM Tris (Tris–MBS) twice, the cells were incubated with or without rabbit anti-dopamine pAb (Chemicon, Temecula, CA, USA) in Tris–MBS containing 0.05% Triton X and FcR-blocking reagent (Miltenyi Biotec) for 30 min at 4°C, followed by FITC-conjugated anti-rabbit IgG (Sigma) for 30 min at 4°C. After washing with Tris–MBS, samples were mounted on cover glasses and visualized with a Radiance 2000 confocal laser scanning microscope (Bio-Rad, Tokyo, Japan) and then were analyzed with a FACSCalibur (BD Biosciences).

Light and electron microscopy

Immature Mo-DCs, stimulated with 10 μM forskolin for 48 h, were fixed as described in the Immunofluorescent detection of dopamine. After being washed with 1% MBS in 50 mM Tris (Tris–MBS) twice, for the preparation of cryostat sections, the cells were cryoprotected with 10% sucrose in Tris–MBS overnight. The cryostat sections (6 μm) were treated with endogenous peroxidase-blocking solution (Dako S2001, Dako, Kyoto, Japan) for 10 min and then were incubated overnight at 4°C with rabbit anti-dopamine polyclonal antibody (Chemicon). After washing with Tris–MBS, the sections were treated with a peroxidase–antiperoxidase streptavidin–biotin conjugating system (Dako K0679; Dako) and then were visualized by conventional light microscopy using liquid diaminobenzidine precipitant (Dako K3465). They were then post-fixed with 2% osmium tetroxide for 1 h, dehydrated in graded series of ethanol and embedded in epoxy resin. When detecting with gold particles, the post-embedding method was performed. Fixed cells were dehydrated in a graded series of ethanol and embedded in LR White resin. Ultrathin sections were blocked for 30 min with 2% skim milk in PBS and then incubated overnight at 4°C with rabbit

anti-dopamine polyclonal antibodies (Chemicon). After washing with PBS, ultrathin sections were treated with anti-rabbit IgG gold conjugate (15 nm, RPN 422V, Amersham) for 60 min, washed with PBS and post-fixed with 2.5% GA. Ultrathin sections were observed by a JEM 1010 electron microscope (JEOL, Tokyo, Japan). The specificity of the above immunoreactivity was confirmed by the substitution of the primary antiserum for PBS.

Measurement of intracellular Ca^{2+}

Intracellular free Ca^{2+} was measured in fura-2-labeled DCs using an AQUACOSMOS system (Hamamatsu Photonics, Shizuoka, Japan) equipped with a Nikon epifluorescence microscope (TE2000-U; Nikon, Tokyo, Japan). Briefly, immature Mo-DCs were incubated with 2 μM fura-2 AM ester (Biotium, Hayward, CA, USA) for 30 min at 37°C in RPMI. The cells were washed twice and re-suspended in RPMI. The fluorescence traces after stimulation were followed fluorospectrometrically, and the ratio between absorption at 340 nm and that at 380 nm was calculated.

Measurement of intracellular cAMP

Immature Mo-DCs and $CD4^+$ naive T cells (10^5 cells per 100 μl in 96-well plates) were incubated at 37°C in PBS containing 0.5% FCS and 1 mM 3-isobutyl-1-methyl-xanthine (nacalai tesque, Kyoto, Japan). After 10 min, dopamine (10^{-6} to 10^{-8} M) was added in the presence or absence of 0.1 μM sulpiride or 1 μM SCH-23390. As a positive control, forskolin (10 μM, Sigma) was used instead. Ten minutes later, to terminate the stimulation and to lyse the cells, cell lysis buffer was added, and the cells were incubated for 10 min. cAMP levels were determined using the CatchPoint™ cyclic-AMP fluorescent assay kit (Molecular Devices, Osaka, Japan), according to the manufacturer's instructions.

Human T-cell clones and the observation of DC–T-cell interaction by time-lapse video microscopy

Human CD4 T-cell clone BC33.5, which recognizes the peptide antigen BCGap84-100 in the context of DRA/DRB1*1405, was established in our previous studies (29, 30). Immature autologous Mo-DCs, stimulated with 10 μM forskolin for 48 h and pulsed with BCGap84-100 peptide, were collected and washed two times with PBS, and 1×10^4 DCs were seeded on a 35-mm glass-base dish (Iwaki, Funabashi, Japan). The dish was placed into a culture chamber on the microscope and maintained at 37°C in a 5% CO_2 atmosphere during observation. The time-lapse images were recorded with Nikon TE2000 inverted phase contrast microscopy (×40 objective lens) equipped with a cooled charge-coupled device camera (ORCA-ER, Hamamatsu Photonics) and AQUACOSMOS imaging system (Hamamatsu Photonics). One minute after the addition of 1×10^5 BC33.5 ($t = 0$), we started to collect images every 30 s for 60 min.

Reverse transcription–PCR analysis of GATA-3 gene expression

HLA-DR-non-shared PBMCs of two healthy individuals were co-cultured to induce a mixed lymphocyte reaction (MLR). Cells were co-cultured with IL-4 (10 ng ml^{-1}) and anti-IFN-γ antibody (10 μg ml^{-1}) or alternatively dopamine alone (0.1 μM). Dopamine was added to culture wells twice a day. Cells were incubated for 3 days, followed by extraction of total RNA using TRIzol Reagent (Invitrogen Life Technologies, Carlsbad, CA, USA). The obtained total RNA was subjected to cDNA synthesis by the SuperScript II RnaseH$^-$ reverse transcriptase (Invitrogen Life Technologies) using oligo (dT) primers. *β-Actin* gene transcripts were amplified as internal controls for the reverse transcription–PCR assay. The sense and anti-sense primers specific for *β-actin* genes were designed as described previously (31). The sense and anti-sense primer sequences specific for *GATA-3* gene were 5′-GAATGCCAATGGGGACCCTG-3′ and 5′-CTAACCCATGGCGGTGACCA-3′, respectively.

DC-mediated T-cell differentiation assay

After washing, immature Mo-DCs were stimulated with the adjuvants to be tested. Two days after the incubation with adjuvants, cellular components were further co-cultured with HLA-DR-non-shared allogeneic $CD4^+$ naive T cells to induce MLR in RPMI 1640 medium supplemented with 10% human serum for 8 days. Thereafter, T cells were re-stimulated with anti-CD3 and anti-CD28 plate-bound antibodies (10 and 1 μg ml^{-1}; BD Pharmingen). Culture supernatants were harvested after 16 h to be subjected to IL-5 and IFN-γ determination by ELISA.

FACS analysis and ELISA

Immature Mo-DCs were incubated for 48 h with 10 μg ml^{-1} LPS, 10 μM forskolin, 10^{-7} M dopamine or 0.1 μM sulpiride. The cells were labeled with anti-CD80 PE and anti-CD86 PE (BD Biosciences) and analyzed using a FACSCalibur flow cytometer and Cell Quest software (BD Biosciences). The culture supernatants were analyzed by ELISA for IL-12p70 (R&D Systems) according to the manufacturer's instructions.

Statistical analysis

Comparisons between sets of two groups were performed using Student's two-tailed *t*-test, while sets of more than two groups were compared by analysis of variance.

Results

Mo-DCs store dopamine

Dopamine is present in lymphocytes, macrophages and neutrophils and is synthesized in these cells from tyrosine via the intermediary L-dopa (21, 32). However, the storage of dopamine in DCs remains obscure. We therefore first investigated the storage of dopamine in human Mo-DCs. Because cAMP-elevating agents can increase the rate of dopamine synthesis and storage via activating TH activity in dopamine-producing cells, we stimulated Mo-DCs with forskolin and stained them for dopamine. Light micrographs revealed that dopamine was abundantly stored in Mo-DCs (Fig. 1A and B). Furthermore, immunoelectron microscopical observation revealed that dopamine is stored in vesicles near the plasma membrane (Fig. 1C–E). These results

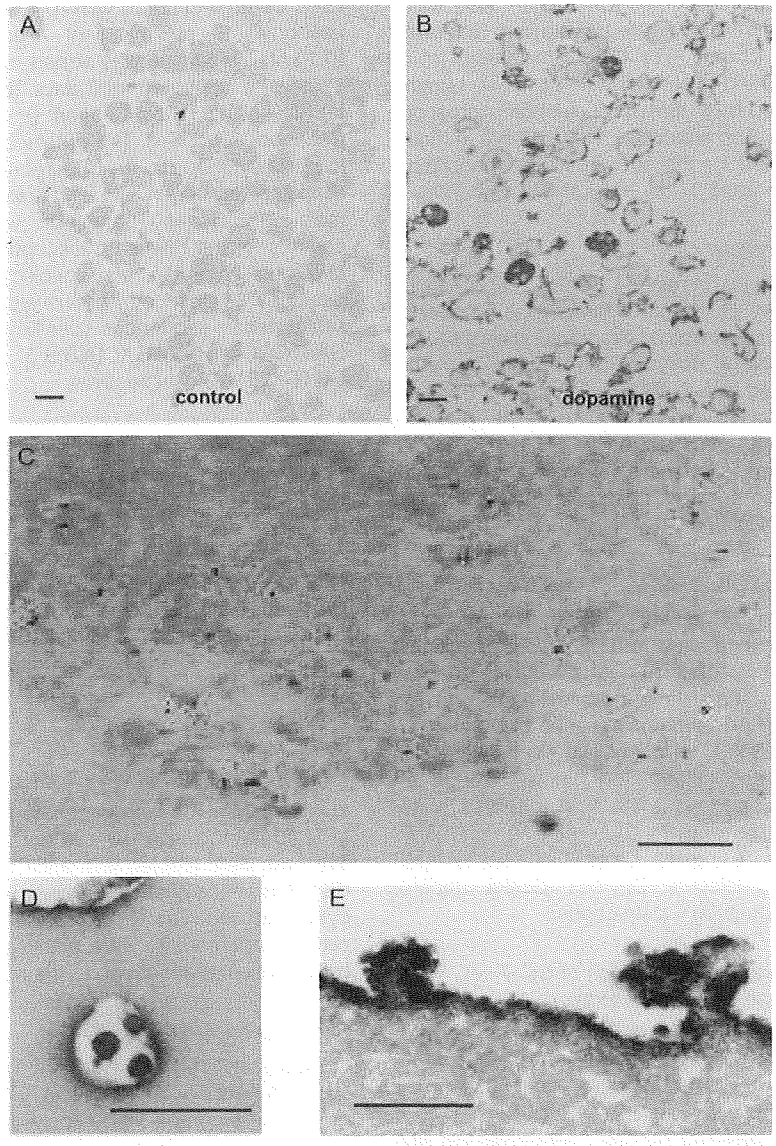

Fig. 1. Immunostaining for dopamine in forskolin-stimulated Mo-DCs. Immature Mo-DCs, stimulated with 10 μM forskolin for 48 h, were fixed and stained as described in the Methods. (A) Light micrographs of control staining. (B) Light micrographs of positive staining. Scale bars, 10 μm. (C–E) Electron micrograph of Mo-DCs. DCs were fixed and labeled with polyclonal anti-dopamine antibody. Antibody was detected with 15-nm gold particles (C) or HRP (D and E). Scale bar, 500 nm.

suggested that Mo-DCs were also able to synthesize and store dopamine in the cells.

Dopamine storage in DCs is regulated by cAMP–TH pathway

We previously reported that Mo-DCs expressed both D1-like and D2-like receptors (28). To evaluate which of the two dopamine receptor subgroups dominantly influence the Mo-DC function, we examined the intracellular Ca^{2+} mobilization and cAMP formation of Mo-DC, in response to exogenously added dopamine. As shown in Fig. 2(A and B), dopamine induced transient Ca^{2+} mobilization and decreased cAMP formation in Mo-DCs. These dopamine-mediated changes were completely inhibited by pretreatment with sulpiride, a selective D2-like antagonist. On the contrary, D1-like antagonists did not exhibit such an inhibitory activity (data not shown). These results suggested that the D2-like receptor is functionally dominant over D1-like receptor in Mo-DCs.

Because dopamine storage was abundant in forskolin-stimulated DCs, we hypothesized that DCs also synthesized dopamine via the cAMP–TH pathway. To examine this hypothesis, we analyzed dopamine storage in Mo-DCs after stimulation with or without forskolin. As shown in Fig. 2(C),

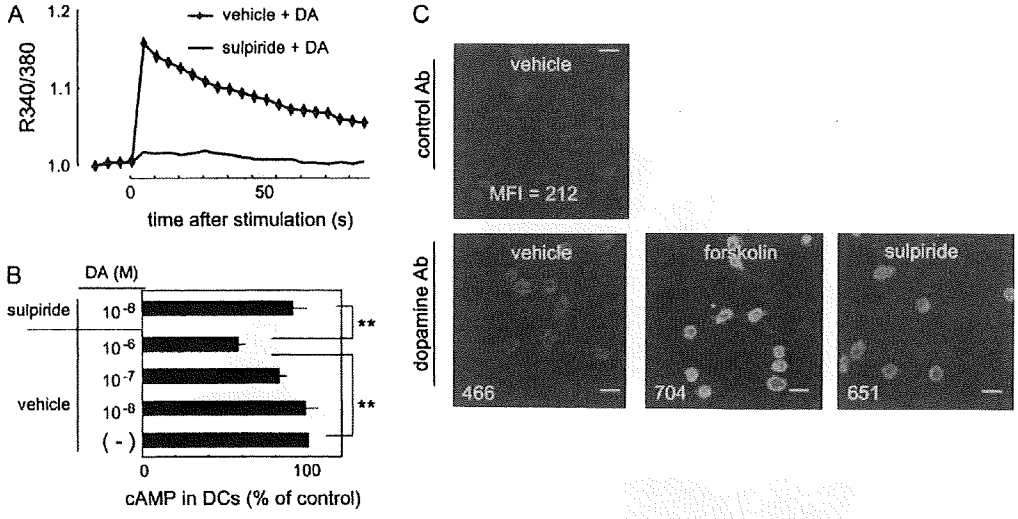

Fig. 2. The regulation of dopamine storage in DCs (A) Intracellular calcium mobilization. Fura-2 AM-loaded Mo-DCs were pre-treated with 0.1 μM sulpiride or vehicle at 37°C for 30 min and were stimulated with 10^{-7} M dopamine. The results are representative of three experiments. (B) cAMP formation in Mo-DCs. Mo-DCs were pre-treated with 3-isobutyl-1-methyl-xanthine and with or without pretreatment with 0.1 μM sulpiride and stimulated with dopamine (10^{-6} to 10^{-8} M). cAMP levels were determined with a cAMP fluorescent assay kit. Each data point represents the percentage of the control (dopamine 0 M). The results are representative of three experiments. Standard deviations are shown as error bars. Statistically significant differences are indicated by asterisks (**$P < 0.01$ versus dopamine 10^{-6} M). (C) Immature Mo-DCs, stimulated with 10 μM forskolin or 0.1 μM sulpiride for 48 h, were fixed and stained as described in the Methods. Indicated numbers are the mean fluorescence intensity analyzed by a FACSCalibur. The results are representative of two experiments. Scale bars, 20 μm.

forskolin increased dopamine storage in Mo-DCs. This result suggested that dopamine storage in Mo-DCs was regulated by the cAMP–TH pathway. In general, dopamine receptors expressed on dopamine-producing cells exist to regulate dopamine synthesis in the cells. D1-like receptors augment the phosphorylation of TH by increasing cAMP and subsequently promote dopamine synthesis. In contrast, D2-like receptors control the phosphorylation of TH by decreasing levels of cAMP, thus resulting in the suppression of dopamine synthesis (33). This means that the signaling balance between D1-like and D2-like receptors regulates dopamine synthesis and storage. We therefore hypothesized that antagonizing D2-like receptors on Mo-DCs increases dopamine storage in Mo-DCs. To test this hypothesis, we analyzed dopamine storage in Mo-DCs after stimulation with a D2-like receptor antagonist sulpiride. As expected, sulpiride also increased dopamine storage in Mo-DCs (Fig. 2C). This phenomenon was observed in Mo-DCs treated with nemonapride, another D2-like receptor antagonist (data not shown). All these results collectively indicate that DCs synthesize dopamine via the cAMP–TH pathway and that antagonizing D2-like receptor increases dopamine synthesis and storage by sustaining the cAMP elevation.

Mo-DCs release dopamine against T cells after antigen-specific DC–T-cell interaction

To examine that dopamine is released by DCs upon interaction with $CD4^+$ T cells, we then observed the interactions between human $CD4^+$ T-cell clone BC33.5, which recognizes BCGap84-100 peptide (29, 30), and immature autologous Mo-DCs stimulated with forskolin in the presence or absence of BCGap84-100 peptide, under time-lapse video microscopy. After dendrite-mediated contact with T cells, many peptide-pulsed DCs, but not non-pulsed DCs, released numerous granules (Fig. 3A). Because dopamine was present at vesicles as granules in Mo-DCs (Fig. 1), this result suggested that these granules released by Mo-DCs contained dopamine. We therefore compared the level of dopamine storage in Mo-DCs before and 2 h after DC–T-cell contact by flow cytometric analysis. As shown in Fig. 3(B), the storage of dopamine in peptide-pulsed DCs after DC–T-cell contact was decreased. These results suggested that antigen-specific interaction with $CD4^+$ T cells enabled Mo-DCs to release dopamine-including vesicles.

T-cell response to dopamine

The D1-like receptors are expressed on both DCs and T cells, whereas D2-like receptors are marginally expressed on $CD4^+CD45RA^+$ naive T cells (28). We then evaluated the cAMP formation within $CD4^+CD45RA^+$ T cells in response to exogenously added dopamine. As shown in Fig. 5(A), dopamine increased cAMP formation in $CD4^+CD45RA^+$ T cells. This dopamine-mediated cAMP elevation in $CD4^+CD45RA^+$ T cells was completely inhibited by the pretreatment with SCH-23390, a selective D1-like antagonist (Fig. 5B). These results suggested that D1-like receptors are functionally dominant in $CD4^+CD45RA^+$ T cells. Because the presence of cAMP-elevating agents at priming reportedly predisposes T cells to differentiate toward the T_h2 phenotype (34–36), we next evaluated IL-4 and IL-5 secretion from $CD4^+CD45RA^+$ T cells which were stimulated by anti-CD3/CD28 antibodies and simultaneously added dopamine. Indeed, dopamine

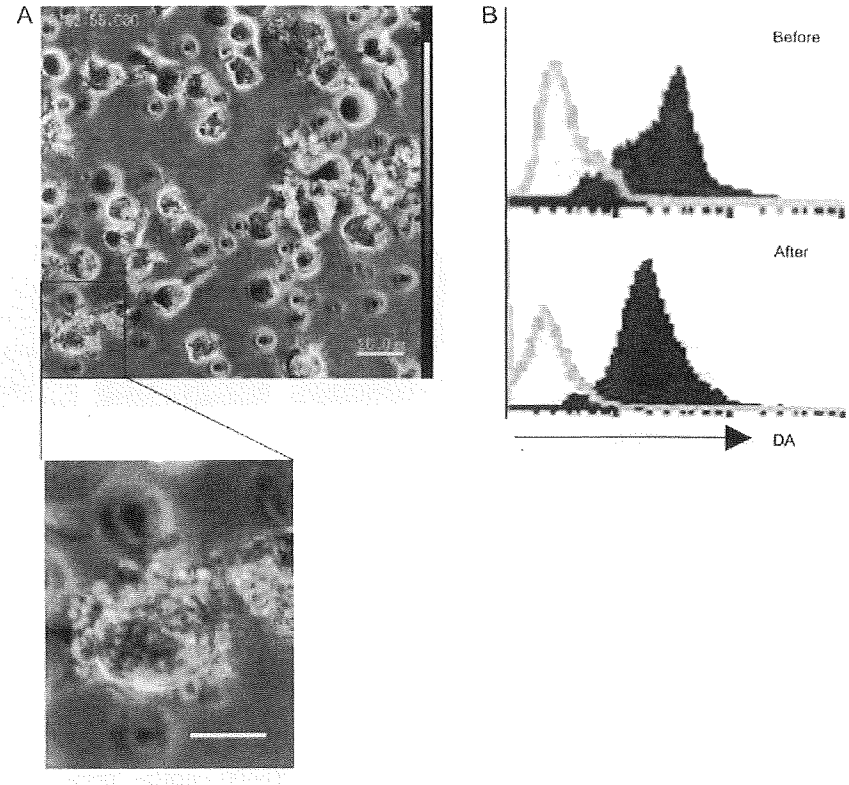

Fig. 3. The interaction between cloned human $CD4^+$ T cells and immature autologous Mo-DCs, stimulated with 10 μM forskolin and pulsed with or without peptide. (A) One representative image of DC–T interaction. The result is from four different movies in two independent experiments. Scale bars, 20 μm. (B) The change of dopamine storage in Mo-DCs. Before (top) and 2 h after (bottom) DC–T-cells co-culturing, dopamine storage in peptide-pulsed DCs was visualized by dopamine staining (filled histograms). Open histograms indicate isotype-matched control IgG. Figures represent three independent experiments.

increased both IL-4 and IL-5 secretion from $CD4^+CD45RA^+$ T cells induced by anti-CD3/CD28 antibodies in a dose-dependent manner (Fig. 5C), indicating that dopamine induced T_h2 polarization via D1-like receptors on naive $CD4^+$ T cells. To determine whether dopamine exhibits GATA-3-inducing activity, we observed *GATA-3* mRNA expression in an MLR, under various conditions. As shown in Fig. 4(D), *GATA-3* expression was significantly increased in an MLR under T_h2-inducing conditions, i.e. in the presence of IL-4 and anti-IFN-γ antibody. Furthermore, addition of dopamine alone in an MLR induced increased *GATA-3* mRNA expression. The series of results suggested that dopamine, synthesized and stored in DCs, was released upon interaction with naive $CD4^+$ T cells, thereby inducing T_h2 polarization, in a mechanism reminiscent of neurotransmission (Fig. 4D). In this sense, DCs and naive T cells correspond to presynaptic neurons and post-synaptic neurons, respectively.

High levels of dopamine released by DCs polarizes T_h2 differentiation

To examine whether or not dopamine emissions from DC influence T_h1–T_h2 differentiation, we checked cytokine profiles and the expression of chemokine receptors such as CXCR3 (as a T_h1-type chemokine receptor) and CCR4 (as a T_h2-type chemokine receptor) in a DC-mediated T cell differentiation assay using human Mo-DCs (37, 38), via stimulation with several chemicals. In this assay system, chemicals were co-incubated with DCs alone; T cells were not exposed to these chemicals. LPS and forskolin were used as positive controls for a T_h1 and a T_h2 adjuvant, respectively. The exposure of DCs to D2-like antagonists, such as sulpiride and nemonapride, led to a high IL-5:IFN-γ ratio (Fig. 5A) and resulted in growth of cells expressing CCR4 and a decrease in cells expressing CXCR3 (Fig. 5B), thus suggesting that antagonizing D2-like receptors on Mo-DCs induced T_h2 polarization when these Mo-DCs were co-cultured with naive T cells. By contrast, SCH-23390 (a specific D1-like antagonist) led to a low IL-5:IFN-γ ratio (Fig. 5C), indicating that D1-like antagonists shift toward T_h1 response. Furthermore, when Mo-DCs were pre-treated with colchicine (a microtubule depolymerizer) to decrease exocytosis, allogeneic naive $CD4^+$ T cells then differentiated into T cells with T_h1-prone cytokine profile (Fig. 5C). D2-like antagonists did not affect the expression levels of CD86 on DCs or IL-12 secretion by DCs (Fig. 5D and E). These results suggested that high levels of dopamine within the DC–naive T-cell junctions induced cAMP production, thereby facilitating T_h2 differentiation. All these findings demonstrated that dopamine released by

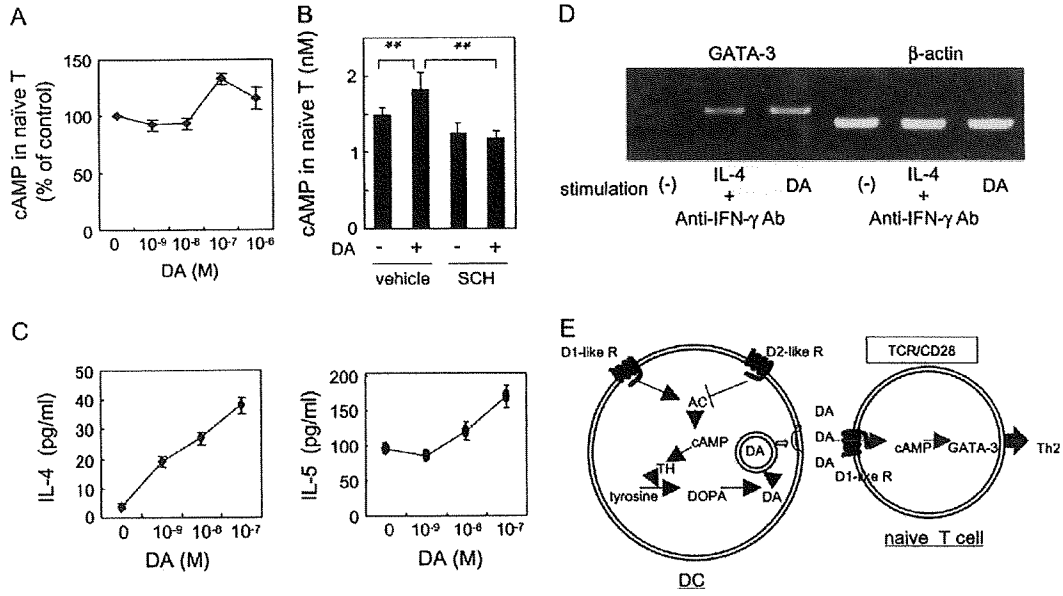

Fig. 4. T-cell response to dopamine (A and B) cAMP formation in naive $CD4^+$ T cells. Naive $CD4^+$ T cells were pre-treated with 3-isobutyl-1-methyl-xanthine and stimulated with dopamine (10^{-6} to 10^{-9} M) (A). Each data point represents the percentage of the control (dopamine 0 M). Naive $CD4^+$ T cells were pre-treated with 3-isobutyl-1-methyl-xanthine and with or without 1 μM SCH-23390 and stimulated with 10^{-7} M dopamine (B). The results are representative of three experiments. Standard deviations are shown as error bars. Statistically significant differences are indicated by asterisks (**$P < 0.01$ versus dopamine 10^{-7} M). (C) IL-4 and IL-5 induction of $CD4^+$ naive T cells. Purified human $CD4^+$ naive T cells were stimulated with anti-CD3 and anti-CD28 plate-bound antibodies and with the indicated concentrations of dopamine. The levels of IL-4 and IL-5 in the culture supernatants after 16 h were determined by ELISA. Standard deviations are shown as error bars. The results are representative of two experiments. (D) GATA3 expression levels induced by an MLR. Cells were co-incubated with IL-4 and anti-IFN-γ antibody, or with 10^{-7} M of dopamine alone, and were subjected to reverse transcription–PCR analysis. (E) A conceptual model for dopamine in DC–naive T-cell interaction. In DC, cAMP–TH pathway may exist and be controlled by dopamine receptors. In DC–naive T interaction, high local concentrations of dopamine released by DC may induce further cAMP formation and IL-5 production.

DCs upon interaction with naive $CD4^+$ T cells, thereby inducing T_h2 polarization.

Discussion

In our current study, we have first demonstrated that DCs, which are ubiquitously distributed in peripheral tissues where they serve as immune sensors, are indeed one of the major sources of dopamine. Human Mo-DCs mainly expressed D1 and D2 among five subtypes of dopamine receptors (28). In human Mo-DCs, the storage of dopamine might be mainly regulated by the signaling balance between D1 and D2 via regulating cAMP formation. Because exogenously added dopamine decreased cAMP formation in Mo-DCs via D2, the expression of D2 on Mo-DCs might function as an autoreceptor led to decreasing the storage of dopamine via decreasing cAMP formation in itself. The D2-like receptor antagonist sulpiride increased dopamine storage in Mo-DCs without the use of dopamine, probably because sulpiride functions as an inverse agonist (39), leading to increasing cAMP formation in Mo-DCs.

Because we focused on the role of dopamine receptors in DC–T-cell interaction in the current study, we did not investigate the uptake of dopamine by dopamine transporters (DATs) and the exocytosis of dopamine. However, levodopa, the metabolic precursor of dopamine, dose dependently increased dopamine storage in Mo-DCs (data not shown), suggesting that Mo-DCs have available DATs. With regard to the exocytotic release of dopamine, DCs released numerous granules in response to ionomycin (10 μM) (data not shown), indicating the association with Ca^{2+} influx. This result suggests that certain molecules expressed on DCs trigger Ca^{2+} influx, leading to the degranulation of dopamine. In the current study, the degranulation needed antigen-specific interaction between DCs and T cells. Initial DC–T-cell adhesion-mediated scanning facilitates recognition of antigen–MHC complexes by the TCR. Several pairs of adhesion molecules are involved in the initial adhesive interactions such as leukocyte function-associated antigen (LFA)-3–CD2, ICAM-1,-3–LFA-1 or DC-SIGN–ICAM-3. Because naive T cells highly express ICAM-3 which can provide co-stimulatory signals to T cells and which has been localized at the APC-T cell interface (40, 41), DC-SIGN–ICAM-3 is thought to be the most important adhesive interaction. The engagement of DC-SIGN by specific antibody triggers PLCγ phosphorylation and Ca^{2+} influx in Mo-DCs (42), suggesting that the adhesive interaction with DC-SIGN–ICAM-3 is able to trigger the exocytosis of dopamine from DCs. Further studies are therefore needed to elucidate these questions.

In dopaminergic neurons, calculated dopamine concentration within 1 ms after unitary synaptic release is 100–250 nM within 1 μm (43). Because the space at DC–T-cell

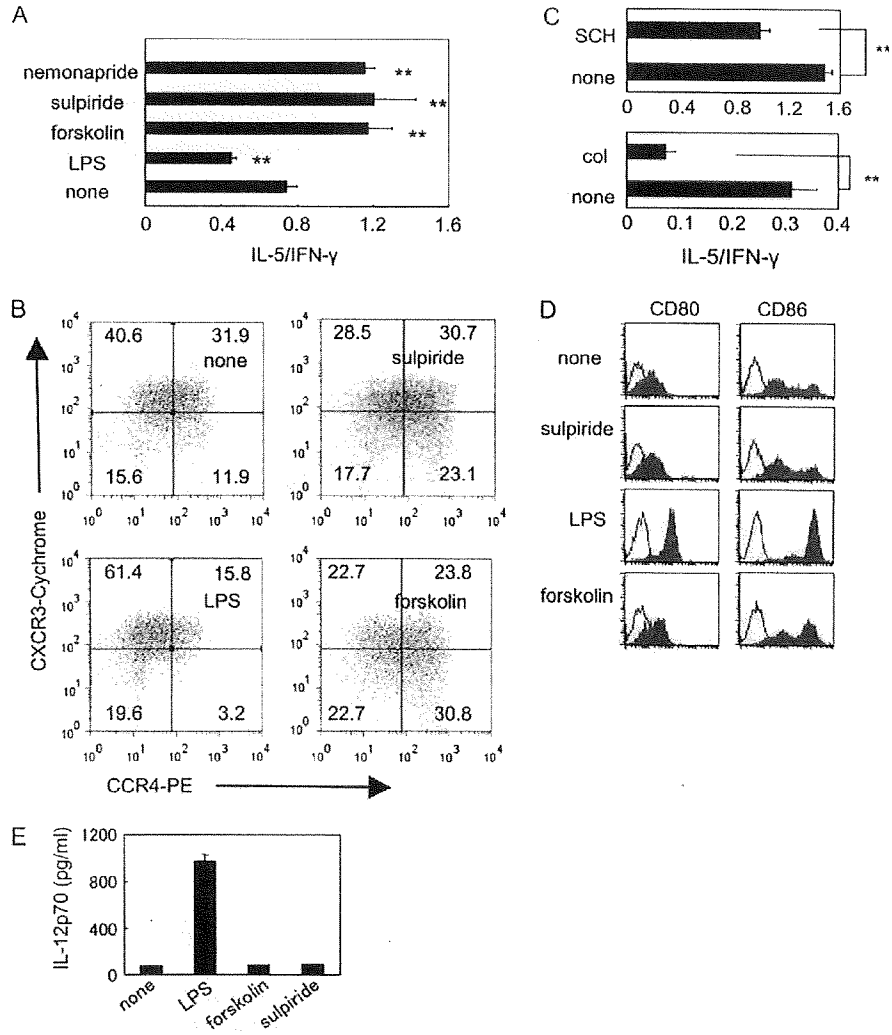

Fig. 5. DC-mediated T_h1–T_h2 differentiation. Immature Mo-DCs were stimulated with indicated chemicals. The cells were subjected to 'DC-mediated T-cell differentiation assay' as described in the Methods. (A and C) Graphs showing IL-5:IFN-γ ratio. Immature Mo-DCs were stimulated with 3 nM nemonapride, 0.1 μM sulpiride, 10 μg ml $^{-1}$ LPS, 10 μM forskolin (A), 1 μM SCH-23390 or 0.5 μg ml $^{-1}$ colhicine (C) for 2 days. Standard deviations are shown as error bars. Statistically significant differences are indicated by asterisks (**$P < 0.01$ versus none). The results are representative of three experiments. (B) Expression of chemokine receptors on T cells. After DC-mediated T-cell differentiation assay, the expression of CXCR3 and CCR4 on T cells was determined by flow cytometry. The percentage of cells in each quadrant is given. (D and E) The effects of dopamine and the D2 antagonist on the surface molecules and IL-12 production of DCs. Immature Mo-DCs were incubated for 48 h with vehicle, 10 μg ml $^{-1}$ LPS, 10 μM forskolin, 10 $^{-7}$ M dopamine or 0.1 μM sulpiride. The cells were stained with mAb to CD80, CD86 (filled histograms) or an isotype control (open histograms) and analyzed by flow cytometry (D). Culture supernatants were analyzed by ELISA for IL-12p70 (E). The results are representative of three experiments.

synapses is within 1 μm (Fig. 3A), the concentration of dopamine in the synapse is estimated to be 100–250 nM, thus indicating that T cells might be exposed to a relatively high concentration of dopamine during DC–T-cell interaction. We have shown that 100 nM is the most effective concentration to induce cAMP formation in naive $CD4^+$ T cells.

We herein demonstrated that dopamine stored in DCs is released upon interaction with naive $CD4^+$ T cells and increases cAMP formation in naive $CD4^+$ T cells, thereby regulating T_h1–T_h2 polarization. In a word, dopamine might function as a T_h2-polarizing factor during DC–naive T-cells interaction. In the DC-mediated T-cell differentiation assay, although we have shown only IL-5:IFN-γ ratio, we have already reported that IL-5:IFN-γ ratio correlated with IL-4:IFN-γ ratio in this assay system (37). DC-mediated T_h2 polarization by D2-like antagonists well corroborates with the observation by others that T_h1 polarization in medication-free schizophrenic patients is attenuated by effective neuroleptic treatment (27). It is also likely from our current results that other substances that affect the cAMP–TH pathway and dopamine storage polarize T_h1–T_h2 differentiation. Indeed, PGE_2 and histamine have been reported to carry T_h2 adjuvant activity (4, 44).

Their receptors belong to the family of seven transmembrane GPCRs, and both PGE_2 and histamine mediate the Gαs–cAMP pathway in Mo-DCs (1, 45). Their T_h2 adjuvant activities have been thought to depend on the suppression of IL-12 secretion from DCs via cAMP formation. However, because they can also up-regulate the cAMP–TH pathway, it is likely that their T_h2 adjuvant activity results from the increased dopamine storage in DCs. In fact, PGE_2 increased the dopamine storage in Mo-DCs as much as forskolin did (data not shown). It is highly likely that the level of dopamine storage in DCs is affected not only by medication but also by microorganisms and environmental chemicals.

Since the discovery of two distinct types of T_h cells (IFN-γ-producing T_h1 cells and IL-4-producing T_h2 cells) in mice by Coffman *et al.* (46), mutual regulation between T_h1 cells and T_h2 cells (T_h1–T_h2 balance) has been considered to be important for homeostatic maintenance of the immune system. For example, dysregulation of the T_h1–T_h2 balance leads to excessive T_h1 cell or T_h2 cell activation, resulting in the development of autoimmune diseases associated with accumulation of T_h1 cells or induction of allergic diseases due to accumulation of T_h2 cells, respectively (47). However, changes in autoimmune diseases that could not be explained by the T_h1–T_h2 paradigm were also observed in several settings: unexpectedly, IFN-γ–IFN-γR deficiency or neutralization resulted in exacerbation, rather than attenuation, of development of autoimmune diseases such as murine encephalomyelitis (48, 49), arthritis (50, 51), uveitis (52, 53) and nephritis (54), which have classically been considered to be T_h1-mediated diseases. Studies for non-T_h1–T_h2 cell-based mechanisms for the pathogenesis of autoimmune diseases identified two additional T_h cell subsets, i.e. IL-17-producing T_h cells (T_h17 cells) and Treg cells. These cells provided new insight into the molecular mechanisms involved in immune responses and/or disease development and led to revision of the classic T_h1–T_h2 paradigm in such settings. We demonstrated that antagonizing D1-like receptors and D2-like receptors polarized T_h1 and T_h2 differentiation, respectively. Moreover, we have recently found that antagonizing D1-like receptors inhibit IL-17-producing T_h cells as well as induce IFN-γ-producing T_h1 cells in murine encephalomyelitis (28). Furthermore, in Treg cells, catecholamine-dependent down-regulation of Treg cells is selectively reversed by antagonizing D1-like receptors (20). Taken all together, antagonizing D1-like receptors may be a useful treatment for several autoimmune diseases and allergic disorders.

In summary, we first demonstrated that DCs synthesize and store dopamine and that dopamine released by DCs is critical for a qualitative fate of T-cell differentiation. We propose that dopamine may therefore play a role in many diseases attributable to an imbalance of T_h cells and that dopamine and dopamine receptors in immune cells can be therapeutic targets.

Funding

Saitama Medical University Internal Grant (18-1-1-06); Research Grant-In-Aid for Scientific Research by the Ministry of Health, Labor and Welfare of Japan, the Ministry of Education, Culture, Sports, Science and Technology of Japan.

Acknowledgements

The authors would like to acknowledge the assistance of K. Utsunomiya with technical advice, T. Egusa for provision of chemicals, S. Ohshima for technical assistance and K. Tanaka and M. Akita for performing electron microscopy. Electron microscopy was performed at the Division of Morphological Science of Biomedical Research Center, Saitama Medical University. The authors declare no financial or commercial conflict of interest.

Abbreviations:

APC	antigen-presenting cell
cAMP	cyclic adenosine 3′,5′-monophosphate
DAT	dopamine transporter
DC	dendritic cell
DC-SIGN	dendritic cell-specific intracellular adhesion molecule-3-grabbing non-integrin
DOPA	dehydroxyphenylalanine
GA	glutaraldehyde
GPCR	G protein-coupled receptors
ICAM	intracellular adhesion molecule
LFA	leukocyte function-associated antigen
MBS	sodium metabisulfite
MLR	mixed lymphocyte reaction
Mo-DC	monocyte-derived dendritic cell
PGE_2	prostaglandin E_2
TH	tyrosine hydroxylase
Treg	regulatory T

References

1 Guermonprez, P., Valladeau, J., Zitvogel, L., Thery, C. and Amigorena, S. 2002. Antigen presentation and T cell stimulation by dendritic cells. *Annu. Rev. Immunol.* 20:621.
2 Kaisho, T. and Akira, S. 2002. Toll-like receptors as adjuvant receptors. *Biochim. Biophys. Acta.* 1589:1.
3 Murphy, K. M., Ouyang, W., Farrar, J. D. *et al.* 2000. Signaling and transcription in T helper development. *Annu. Rev. Immunol.* 18:451.
4 Caron, G., Delneste, Y., Roelandts, E. *et al.* 2001. Histamine polarizes human dendritic cells into Th2 cell-promoting effector dendritic cells. *J. Immunol.* 167:3682.
5 Kalinski, P., Schuitemaker, J. H. N., Hilkens, C. M. U. and Kapsenberg, M. L. 1998. Prostaglandin E2 induces the final maturation of IL-12-deficient CD1a+CD83+ dendritic cells: the levels of IL-12 are determined during the final dendritic cell maturation and are resistant to further modulation. *J. Immunol.* 161:2804.
6 Mazzoni, A., Young, H. A., Spitzer, J. H., Visintin, A. and Segal, D. M. 2001. Histamine regulates cytokine production in maturing dendritic cells, resulting in altered T cell polarization. *J. Clin. Invest.* 108:1865.
7 Kuchroo, V. K., Das, M. P., Brown, J. A. *et al.* 1995. B7-1 and B7-2 costimulatory molecules activate differentially the Th1/Th2 developmental pathways: application to autoimmune disease therapy. *Cell* 80:707.
8 Freeman, G. J., Boussiotis, V. A., Anumanthan, A. *et al.* 1995. B7-1 and B7-2 do not deliver identical costimulatory signals, since B7-2 but not B7-1 preferentially costimulates the initial production of IL-4. *Immunity* 2:523.
9 Gutzmer, R., Diestel, C., Mommert, S. *et al.* 2005. Histamine H4 receptor stimulation suppresses IL-12p70 production and mediates chemotaxis in human monocyte-derived dendritic cells. *J. Immunol.* 174:5224.
10 Harizi, H., Juzan, M., Pitard, V., Moreau, J.-F. and Gualde, N. 2002. Cyclooxygenase-2-issued prostaglandin E2 enhances the production of endogenous IL-10, which down-regulates dendritic cell functions. *J. Immunol.* 168:2255.
11 Norcross, M. A., Bentley, D. M., Margulies, D. H. and Germain, R. N. 1984. Membrane Ia expression and antigen-presenting accessory cell function of L cells transfected with class II major histocompatibility complex genes. *J. Exp. Med.* 160:1316.

12 Dustin, M. L. and Cooper, J. A. 2000. The immunological synapse and the actin cytoskeleton: molecular hardware for T cell signaling. *Nat. Immunol.* 1:23.
13 O'Connell, P. J., Wang, X., Leon-Ponte, M., Griffiths, C., Pingle, S. C. and Ahern, G. P. 2006. A novel form of immune signaling revealed by transmission of the inflammatory mediator serotonin between dendritic cells and T cells. *Blood* 107:1010.
14 Pacheco, R., Oliva, H., Martinez-Navio, J. M. *et al.* 2006. Glutamate released by dendritic cells as a novel modulator of T cell activation. *J. Immunol.* 177:6695.
15 Roskoski, R. Jr and Roskoski, L. M. 1987. Activation of tyrosine hydroxylase in PC12 cells by the cyclic GMP and cyclic AMP second messenger systems. *J. Neurochem.* 48:236.
16 Missale, C., Nash, S. R., Robinson, S. W., Jaber, M. and Caron, M. G. 1998. Dopamine receptors: from structure to function. *Physiol. Rev.* 78:189.
17 Basu, S. and Dasgupta, P. S. 2000. Dopamine, a neurotransmitter, influences the immune system. *J. Neuroimmunol.* 102:113.
18 Meredith, E. J., Chamba, A., Holder, M. J., Barnes, N. M. and Gordon, J. 2005. Close encounters of the monoamine kind: immune cells betray their nervous disposition. *Immunology* 115:289.
19 Bergquist, J., Tarkowski, A., Ekman, R. and Ewing, A. 1994. Discovery of endogenous catecholamines in lymphocytes and evidence for catecholamine regulation of lymphocyte function via an autocrine loop. *Proc. Natl Acad. Sci. USA* 91:12912.
20 Cosentino, M., Fietta, A. M., Ferrari, M. *et al.* 2007. Human CD4+CD25+ regulatory T cells selectively express tyrosine hydroxylase and contain endogenous catecholamines subserving an autocrine/paracrine inhibitory functional loop. *Blood* 109:632.
21 Flierl, M. A., Rittirsch, D., Nadeau, B. A. *et al.* 2007. Phagocyte-derived catecholamines enhance acute inflammatory injury. *Nature* 449:721.
22 Abi-Dargham, A., Rodenhiser, J., Printz, D. *et al.* 2000. From the cover: increased baseline occupancy of D2 receptors by dopamine in schizophrenia. *Proc. Natl Acad. Sci. USA* 97:8104.
23 Seeman, P. and Niznik, H. B. 1990. Dopamine receptors and transporters in Parkinson's disease and schizophrenia. *FASEB J.* 4:2737.
24 Ilani, T., Ben-Shachar, D., Strous, R. D. *et al.* 2001. A peripheral marker for schizophrenia: increased levels of D3 dopamine receptor mRNA in blood lymphocytes. *Proc. Natl Acad. Sci. USA* 98:625.
25 Boneberg, E. M., von Seydlitz, E., Propster, K., Watzl, H., Rockstroh, B. and Illges, H. 2006. D3 dopamine receptor mRNA is elevated in T cells of schizophrenic patients whereas D4 dopamine receptor mRNA is reduced in CD4+ -T cells. *J. Neuroimmunol.* 173:180.
26 Kim, Y. K., Myint, A. M., Lee, B. H. *et al.* 2004. Th1, Th2 and Th3 cytokine alteration in schizophrenia. *Prog. Neuropsychopharmacol. Biol. Psychiatry* 28:1129.
27 Avgustin, B., Wraber, B. and Tavcar, R. 2005. Increased Th1 and Th2 immune reactivity with relative Th2 dominance in patients with acute exacerbation of schizophrenia. *Croat. Med. J.* 46:268.
28 Nakano, K., Higashi, T., Hashimoto, K., Takagi, R., Tanaka, Y. and Matsushita, S. 2008. Antagonizing dopamine D1-like receptor inhibits Th17 cell differentiation: preventive and therapeutic effects on experimental autoimmune encephalomyelitis. *Biochem. Biophys. Res. Commun.* 373:286.
29 Matsushita, S., Kohsaka, H. and Nishimura, Y. 1997. Evidence for self and nonself peptide partial agonists that prolong clonal survival of mature T cells *in vitro*. *J. Immunol.* 158:5685.
30 Matsushita, S., Yokomizo, H., Kohsaka, H. and Nishimura, Y. 1996. Diversity of a human CD4+ T cell repertoire recognizing one TCR ligand. *Immunol. Lett.* 51:191.
31 Dong, L., Chen, M., Zhang, Q., Li, L. Z., Xu, X. Q. and Xiao, W. 2006. T-bet/GATA-3 ratio is a surrogate measure of Th1/Th2 cytokine profiles and may be novel targets for CpG ODN treatment in asthma patients. *Chin. Med. J.* 119:1396.
32 Gordon, J. and Barnes, N. M. 2003. Lymphocytes transport serotonin and dopamine: agony or ecstasy? *Trends Immunol.* 24:438.
33 Salah, R. S., Kuhn, D. M. and Galloway, M. P. 1989. Dopamine autoreceptors modulate the phosphorylation of tyrosine hydroxylase in rat striatal slices. *J. Neurochem.* 52:1517.
34 Klein-Hessling, S., Jha, M. K., Santner-Nanan, B. *et al.* 2003. Protein kinase A regulates GATA-3-dependent activation of IL-5 gene expression in Th2 cells. *J. Immunol.* 170:2956.
35 Roy, S., Wang, J., Charboneau, R., Loh, H. H. and Barke, R. A. 2005. Morphine induces CD4+ T cell IL-4 expression through an adenylyl cyclase mechanism independent of the protein kinase A pathway. *J. Immunol.* 175:6361.
36 Suarez, A., Mozo, L. and Gutierrez, C. 2002. Generation of CD4+CD45RA+ effector T cells by stimulation in the presence of cyclic adenosine 5′-monophosphate-elevating agents. *J. Immunol.* 169:1159.
37 Wakui, M., Nakano, K. and Matsushita, S. 2007. Notch ligand mRNA levels of human APCs predict Th1/Th2-promoting activities. *Biochem. Biophys. Res. Commun.* 358:596.
38 Higashi, T., Wakui, M., Nakano, K. *et al.* 2008. Evaluation of adjuvant activities using human antigen presenting cells *in vitro*. *Allergol. Int.* 57:219.
39 Strange, P. G. 2001. Antipsychotic drugs: importance of dopamine receptors for mechanisms of therapeutic actions and side effects. *Pharmacol. Rev.* 53:119.
40 Grakoui, A., Bromley, S. K., Sumen, C. *et al.* 1999. The immunological synapse: a molecular machine controlling T cell activation. *Science* 285:221.
41 Montoya, M. C., Sancho, D., Bonello, G. *et al.* 2002. Role of ICAM-3 in the initial interaction of T lymphocytes and APCs. *Nat. Immunol.* 3:159.
42 Caparros, E., Munoz, P., Sierra-Filardi, E. *et al.* 2006. DC-SIGN ligation on dendritic cells results in ERK and PI3K activation and modulates cytokine production. *Blood* 107:3950.
43 Wickens, J. R. and Arbuthnott, G. W. 2005. Structural and functional interactions in the striatum at the receptor level. In Dunnet, S. B., Bentivoglio, M., Bjorklund, A. and Hokfelt, T., eds, *Handbook of Chemical Neuroanatomy*, p. 199. Elsevier Science Publishing Co., Amsterdam, The Netherlands.
44 McIlroy, A., Caron, G., Blanchard, S. *et al.* 2006. Histamine and prostaglandin E up-regulate the production of Th2-attracting chemokines (CCL17 and CCL22) and down-regulate IFN-gamma-induced CXCL10 production by immature human dendritic cells. *Immunology* 117:507.
45 Harizi, H., Grosset, C. and Gualde, N. 2003. Prostaglandin E2 modulates dendritic cell function via EP2 and EP4 receptor subtypes. *J. Leukoc. Biol.* 73:756.
46 Mosmann, T., Cherwinski, H., Bond, M., Giedlin, M. and Coffman, R. 1986. Two types of murine helper T cell clone. I. Definition according to profiles of lymphokine activities and secreted proteins. *J. Immunol.* 136:2348.
47 Bach, J. F. 2002. The effect of infections on susceptibility to autoimmune and allergic diseases. *N. Engl. J. Med.* 347:911.
48 Krakowski, M. and Owens, T. 1996. Interferon-gamma confers resistance to experimental allergic encephalomyelitis. *Eur. J. Immunol.* 26:1641.
49 Willenborg, D. O., Fordham, S., Bernard, C. C., Cowden, W. B. and Ramshaw, I. A. 1996. IFN-gamma plays a critical down-regulatory role in the induction and effector phase of myelin oligodendrocyte glycoprotein-induced autoimmune encephalomyelitis. *J. Immunol.* 157:3223.
50 Manoury-Schwartz, B., Chiocchia, G., Bessis, N. *et al.* 1997. High susceptibility to collagen-induced arthritis in mice lacking IFN-gamma receptors. *J. Immunol.* 158:5501.
51 Vermeire, K., Heremans, H., Vandeputte, M., Huang, S., Billiau, A. and Matthys, P. 1997. Accelerated collagen-induced arthritis in IFN-gamma receptor-deficient mice. *J. Immunol.* 158:5507.
52 Caspi, R., Chan, C., Grubbs, B. *et al.* 1994. Endogenous systemic IFN-gamma has a protective role against ocular autoimmunity in mice. *J. Immunol.* 152:890.
53 Jones, L., Rizzo, L., Agarwal, R. *et al.* 1997. IFN-gamma-deficient mice develop experimental autoimmune uveitis in the context of a deviant effector response. *J. Immunol.* 158:5997.
54 Ring, G. H., Dai, Z., Saleem, S., Baddoura, F. K. and Lakkis, F. G. 1999. Increased susceptibility to immunologically mediated glomerulonephritis in IFN-{gamma}-deficient mice. *J. Immunol.* 163:2243.

FEBS Letters 584 (2010) 61–66

FEBS Letters

journal homepage: www.FEBSLetters.org

Advanced glycation end products increase endothelial permeability through the RAGE/Rho signaling pathway

Akiko Hirose, Takahisa Tanikawa, Hiroko Mori, Yosuke Okada, Yoshiya Tanaka *

First Department of Internal Medicine, School of Medicine, University of Occupational and Environmental Health, 1-1 Iseigaoka, Yahatanishi-ku, Kitakyushyu 807-8555, Japan

ARTICLE INFO

Article history:
Received 17 September 2009
Revised 16 November 2009
Accepted 17 November 2009
Available online 26 November 2009

Edited by Lukas Huber

Keywords:
AGE
Rho
Permeability
Actin
Endothelial cell
Diabetes mellitus

ABSTRACT

Although increased vascular permeability is known to be a major characteristic of diabetic vasculopathy, the precise mechanisms and relevance of advanced glycation end products (AGE) to hyperpermeability of vessels remains unclear. Here, we studied changes in cytoskeletal configuration and the signaling mechanism induced by AGE in human endothelial cells. AGE-BSA stimulation induced Rho activation, intercellular gap formation, prominent actin stress fiber and cell contraction without changing VE-cadherin, and subsequently transendothelial diffusion of FITC-labeled dextran. These processes induced by AGE-BSA were inhibited by either Rho-kinase inhibitor Y27632 or anti-RAGE antibody. We also showed that RhoA and RAGE spontaneously formed a complex. These findings suggest that activation of RAGE/Rho is involved in AGE-BSA-induced hyperpermeability through gap formation and actin reorganization in diabetes.

Structured summary:
MINT-7301170: *Rhotekin* (uniprotkb:Q9BST9) *physically interacts* (MI:0915) with *RhoA* (uniprotkb:P61586) by *pull down* (MI:0096)
MINT-7301204, MINT-7301186: *RhoA* (uniprotkb:P61586) *physically interacts* (MI:0915) with *RAGE* (uniprotkb:Q15109) by *anti bait coimmunoprecipitation* (MI:0006)

1. Introduction

Diabetic mellitus is a chronic progressive disease associated with serious complication including various vasculopathies. Increased capillary permeability occurs in the early stages of diabetes before the onset of structural angiopathy and is known to be a major characteristic of diabetic vasculopathy [1–4]. However, little is known about the intracellular signals that propagate these endothelial structural changes and lead to hyperpermeability during pathological processes of diabetes.

Endothelial structural changes, weak or loss of adherence junction, cell contraction, and focal adhesion redistribution are considered involved in hyperpermeability induced by various insults such as inflammatory stimuli [5]. Previous studies also reported the disorganization of tight junction structures in diabetic retina and cerebral microvessels [6], suggesting that these abnormalities could explain diabetic hyperpermeability. Another studies indicated that high glucose induces actin stress fiber formation in endothelial cells [7] and that microvascular leakage in the retinal microvasculature is enhanced in STZ-induced diabetic rats with high levels of F-actin stress fibers [8], suggesting a relation between hyperglycemia and cytoskeletal contraction, which leads to hyperpermeability.

Accumulated evidence indicates that advanced glycation end products (AGEs) increase at an accelerated rate in diabetes and in parallel with the severity of diabetic complications [9]. AGEs activate RAGEs, a major receptor for AGEs, modulate various cell functions and play a role in vasculopathies through multiple intracellular signal transduction pathways, including p21ras, MAP kinases, PI3 kinase and many [4,10]. However, the relationship AGE with the receptor and the following signaling pathways was unclear. In this study to clarify the signaling mechanism that lead to papillary hyperpermeability in diabetes, we investigated changes in cytoskeletal configuration induced by AGE and the role of the RAGE/Rho signaling pathway in AGE-mediated microvascular hyperpermeability using human vascular endothelial cells in vitro.

2. Materials and methods

2.1. Antibodies and materials

Mouse monoclonal antibodies (mAb) to human VE-cadherin and human RAGE were purchased from R&D Systems (Minneapolis, MN).

* Corresponding author. Fax: +81 93 691 9334.
E-mail address: tanaka@med.uoeh-u.ac.jp (Y. Tanaka).

0014-5793/$36.00 © 2009 Federation of European Biochemical Societies. Published by Elsevier B.V. All rights reserved.
doi:10.1016/j.febslet.2009.11.082

Mouse mAb to human RhoA was from Santa Cruz Biotechnology (Santa Cruz, CA), mouse mAb to human β-actin was from Sigma (St. Louis, MO), and horseradish peroxidase-conjugated horse anti-mouse secondary antibody was from Amersham Biosciences (Arlington Heights, IL). Rhodamine–phalloidin and Alexa Fluor 488-conjugated goat anti-mouse secondary antibody were purchased from Invitrogen (Carlsbad, CA). AGE-bovine serum albumin (BSA) was purchased from BioVision (Mountain View, CA), BSA was from Sigma. Rho-kinase inhibitor Y27632 was obtained from Biomol (Plymouth Meeting, PA).

2.2. Cell culture

Human umbilical vein endothelial cells (HUVECs) were obtained from Cambrex (Walkersville, MD) and cultured in EGM-2 (Lonza) complete medium containing 2% (v/v) fetal bovine serum (FBS), multiple recombinant human growth factors including vascular endothelial growth factor (VEGF), fibroblast growth factor (FGF), insulin growth factor-1 (IGF1), and epidermal growth factor, as well as hydrocortisone, heparin, and ascorbic acid. Experiments were performed using cells up to passage 3. Where appropriate, cells were starved in serum-free basal EBM-2 (Lonza) medium prior to treatment.

2.3. Endothelial monolayer permeability assay

HUVEC were plated in 24-well Transwell units (with polycarbonate membrane, 8-μm pores; Nunc) pre-coated with fibronectin (2.5 μg/well) and cultured to confluence in EGM-2. At the start of the experiment, the culture medium in the lower and upper compartments was replaced with EBM-2 containing AGE-BSA or control BSA. After incubation, FITC-labeled dextran (initial concentration 400 μg/ml) was added to the upper compartment. After 1 h of additional incubation at 37 °C, the medium in the lower compartments was collected and analyzed in a fluorescence detector using 485 nm and 538 nm as the excitation and emission wavelengths, respectively.

2.4. Fluorescent staining of F-actin and VE-cadherin

HUVECs were plated in glass-bottom 35-mm dishes pre-coated with fibronectin (2.5 μg/well) and cultured to confluence in EGM-2. At the start of the experiment, the culture medium was replaced with EBM-2 containing AGE-BSA or control BSA. After incubation, the cells were fixed in 3.7% formaldehyde solution for 3 min and permeabilized with 0.1% Triton X-100 for 3 min. They were then incubated with rhodamine–phalloidin for 20 min in room temperature to stain F-actin. For staining VE-cadherin, cells were fixed in 3.7% formaldehyde solution for 10 min then incubated with mAbs against VE-cadherin at room temperature for 1 h, followed by Alexa Fluor 488-conjugated secondary antibody at room temperature in the dark for 1 h. Fluorescence was detected with a Zeiss Axiophot microscope.

2.5. Western blotting

HUVECs were cultured in cell culture dishes to confluence. Cells were starved in serum-free medium for 1 h and then exposed to BSA or AGE-BSA (50 μg/ml) for different times as indicated. Cell extracts were prepared with a lysis buffer as previously described [11]. Protein concentration was determined with Bradford reaction.

2.6. Rho activation assay

Rho activation was determined by a pull-down assay using GST-Rhotekin-Rho-binding domain (GST-RBD). HUVEC were cultured in cell culture dishes to confluence. Cells were starved in serum-free medium for 6 h and then exposed to AGE-BSA (50 μg/ml) or BSA (50 μg/ml) for different times as indicated, quickly washed with ice-cold Tris-buffered saline, and lysed in 500 μl of lysis buffer. Cell lysates were immediately centrifuged at 8000 rpm at 4 °C for 5 min and equal volumes of lysates were incubated with 30 μg GST-RBD beads for 1 h at 4 °C. The beads were washed with wash buffer, and bound Rho was eluted by boiling each sample in Laemmli sample buffer. Eluted samples from the beads and total cell lysate were then electrophoresed on 15% SDS–polyacrylamide gel electrophoresis gels, transferred to nitrocellulose, blocked with 5% non-fat milk, and analyzed by Western blotting using a polyclonal anti-Rho antibody.

2.7. Immunoprecipitation

Immunoprecipitations were carried out utilizing RhoA or RAGE antibodies. HUVEC were cultured in cell dishes to confluence. Cells were starved in serum-free medium for 6 h and then exposed to AGE-BSA (50 μg/ml) or serum-free medium only for 10 min, quickly washed with ice-cold Tris-buffered saline, and lysed in 500 μl of lysis buffer. Cell lysates were immediately centrifuged at 8000 rpm at 4 °C for 5 min. The supernatants were incubated end-over-end for 60 min at 4 °C with the mixture with Protein G sepharose beads, which were incubated end-over-end for 30 min at 4 °C with anti-RAGE antibody (5 μg/ml) or anti-RhoA antibody (5 μg/ml). The beads were washed three times with PBS-T, then treated with elution buffer (2.5% acetic acid), and the eluted immunoprecipitated samples were resuspended in Laemmli buffer and heated at 100 °C for 3 min, and analyzed by SDS–PAGE, transferred to nitrocellulose, blocked with 5% non-fat milk, and analyzed by Western blotting using a monoclonal anti-Rho antibody or anti-RAGE antibody.

2.8. Statistical analysis

All data were obtained from at least five independent experiments performed in triplicate. Results were expressed as means ± S.D. Analyses of differences were carried out by ANOVA followed by posthoc Student Newman Keuls test. A P value < 0.05 was considered statistically significant.

3. Results

3.1. AGE-BSA increases endothelial permeability

First, we investigated the effect of AGEs on permeability of human endothelial cells by observing diffusion of dextran in HUVEC. AGE-BSA increased transendothelial diffusion of FITC-labeled dextran in a time-dependent and a dose-dependent manner, whereas unmodified BSA had no effect on the permeability (Fig. 1A and B). These findings suggest AGE-BSA have a potential to induce endothelial permeability and disturb the physiological barrier of capillary endothelium.

3.2. AGE-BSA causes intercellular gap formation and reorganization of actin cytoskeleton

To test whether AGEs-induced changes in permeability are due to morphological changes in the endothelial cells, we stained actin and VE-cadherin in endothelial cells treated with or without AGE-BSA. While control cells and cells treated with BSA showed cobblestone morphology without intercellular gap, endothelial cells treated with AGE-BSA showed intercellular gap formation (Fig. 2A-a). Next, we focused on the changes in the cytoskeleton. Although

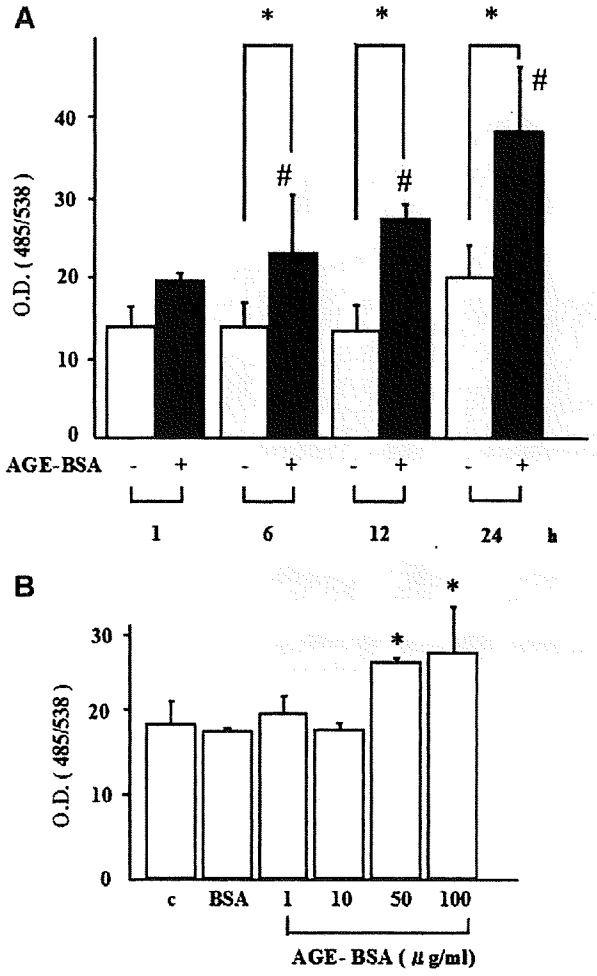

Fig. 1. AGE-BSA perturbed the endothelial barrier of cultured HUVEC monolayers. (A) HUVEC on Transwell inserts were incubated with 50 μg/ml AGE-BSA for the indicated time periods. (B) HUVEC on Transwell inserts were incubated for 6 h with AGE-BSA at various doses or BSA. After incubation, FITC-labeled dextran was added to the upper compartment. After 1 h of additional incubation at 37 °C, the medium in the lower compartment was collected for fluorometric analysis. AGE-BSA increased transendothelial diffusion of FITC-labeled dextran in time- and dose-dependent manners. Unmodified BSA had no effect on monolayer permeability. Data are expressed as means ± S.D. ($n = 3$). $^{*}P < 0.05$ vs. control for each time period. $^{\#}P < 0.05$, compared with the group treated with AGE-BSA (−) for 1 h (A). $^{*}P < 0.05$ vs. control (B).

control cells and cells treated with BSA showed peripheral actin ring, but lacked with stress fibers, the cells treated with AGE-BSA showed prominent actin stress fiber and cell contraction (Fig. 2A-b). We also examined the protein level of VE-cadherin in HUVECs by Western blotting, but treatment with AGE-BSA for the indicated time periods did not modify the level of VE-cadherin (Fig. 2B).

3.3. AGE-BSA activates Rho and RhoA forms a complex with RAGE on HUVECs

To investigate whether these actin rearrangements induced by AGE-BSA are involved in the activation of Rho–Rho kinase, we measured Rho activation in HUVECs by pull-down assay using GST-Rhotekin-Rho-binding domain (GST-RBD). AGE-BSA stimulation increased the amount of activated Rho in HUVECs in a time-dependent manner (Fig. 3A-a). BSA stimulation for the indicated time periods did not modify the amount of activated Rho (Fig. 3A-b). These results suggest that AGE-BSA induces Rho activation in HUVECs. To investigate whether Rho is bound to RAGE, we carried out immunoprecipitation experiments using RhoA and RAGE antibodies. As shown in Fig. 3B, RhoA formed a complex with RAGE on HUVECs with or without AGE-BSA stimulation.

3.4. Rho/Rho kinase inhibitor and anti-RAGE antibody inhibits AGE-BSA-induced cell contraction with actin reorganization and transendothelial hyperpermeability

To investigate whether these morphological changes induced by AGE-BSA are due to activation of Rho/Rho kinase, we pretreated the cells with the Rho kinase inhibitor Y27632 (1 h, 10 μM) and then stimulated the cells with AGE-BSA. As shown in Fig. 4A, Y27632 completely blocked the AGE-BSA-induced gap formation with actin reorganization. To investigate whether these changes induced by AGE-BSA are mediated through AGE–RAGE interaction, we pretreated cells with anti-RAGE antibody for 1 h and then stimulated the cells with AGE-BSA. Anti-RAGE antibody blocked AGE-BSA induced gap formation with actin reorganization. Y27632 or anti-RAGE antibody also blocked the AGE-BSA induced increase in endothelial cell permeability. These findings suggest that activation of RAGE/Rho is involved in AGE-BSA induced hyperpermeability through gap formation and actin reorganization.

4. Discussion

Previous studies proposed various mechanisms for the increased microvascular permeability in diabetic mellitus. Endothelial structural changes, weak or loss of adherence junction, cell contraction, and focal adhesion redistribution are considered involved in hyperpermeability induced by various insults such as inflammatory stimuli [5]. However, apart from these endothelial structural changes, little is known about the intracellular signals that propagate these endothelial structural changes and lead to hyperpermeability. Our study focused on the effect of AGEs on vascular hyperpermeability. AGEs are thought to modulate various cell functions and play a role in vasculopathies and found the following a sequence of results; RhoA and RAGE spontaneously formed a complex, AGE-BSA induced Rho activation, intercellular gap formation, reorganization of actin stress fiber and cell contraction, AGE-BSA induced transendothelial diffusion of FITC-labeled dextran implying its hyperpermeability. However, our results showed no changes in VE-cadherin.

It is well known that activation of RAGEs by AGEs transduces multiple intracellular signal transduction pathways, including p21ras, MAP kinases, PI3 kinase, NAD(P)H oxidase, and results in activation of nuclear factor-kappaB (NF-κB) [10]. Another study also reported that AGEs induced hyperpermeability through actin rearrangement via ERK and p38 MAPK pathways [4]. However the relationship with the receptor of AGE and these signaling pathways was unclear. On the other hand, little is known about AGEs and small G protein. Although it was reported that activation of RAGEs by AGEs induced neurite outgrowth through the cdc42/Rac pathway [12], the relation between actin polymerization induced by AGEs and Rho signaling is not clear. In this study, we investigated the role of the Rho signaling pathway in AGE-mediated microvascular hyperpermeability. Rho is a major small GTP-binding protein and acts a molecular switch that controls a large variety of signal transduction pathways, many of which regulate actin cytoskeleton remodeling in various types of cells. Rho relays extracellular signals to a large number of downstream effectors. Therefore, Rho is a very important signaling element that cooperates with other small GTP-proteins to regulate various cell

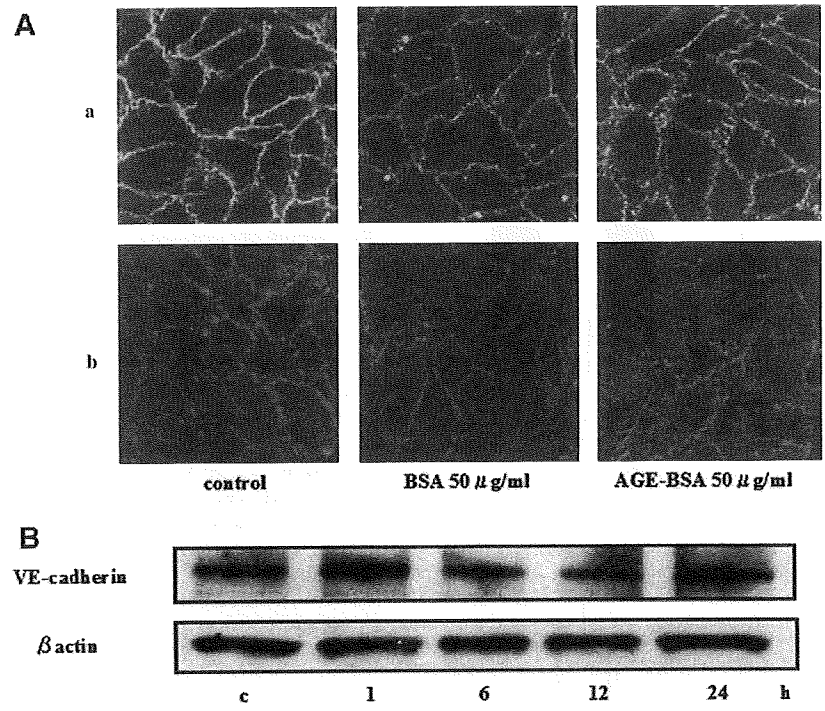

Fig. 2. AGE-BSA induced intercellular gap formation with reorganization of actin cytoskeleton, but no changes in total cellular level of VE cadherin. (A) HUVECs grown on fibronectin-coated glass-bottom dishes were treated with 50 μg/ml AGE-BSA or BSA. After 6 h, cells were fixed and processed for immunofluorescence analysis of VE-cadherin (a) and actin (b). HUVEC treated with AGE-BSA showed gap formation and reorganization of the actin cytoskeleton. Untreated control cells or HUVEC treated with BSA showed no gap formation or stress fiber. (B) HUVECs were treated for the indicated time periods with 50 μg/ml AGE-BSA. After washing, cells were extracted with lysis buffer. Immunoprecipitated VE-cadherin and actin were detected using specific antibodies. Treatment with AGE-BSA for the indicated time periods did not modify the level of VE-cadherin protein. Representative results of five experiments performed with similar results.

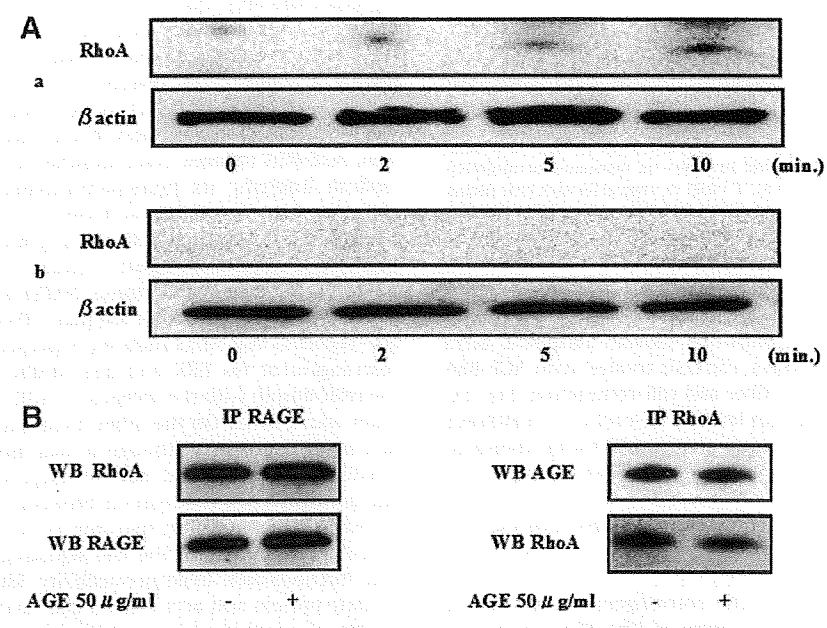

Fig. 3. AGE-BSA activated Rho and RhoA forms a complex with RAGE on HUVECs. (A) HUVECs were treated with 50 μg/ml AGE-BSA (a) or BSA (b) as indicated time. After washing, cells were extracted with lysis buffer. Cell lysates were incubated with GST-RBD beads and RBD-bound Rho were eluted and immunoprecipitated with polyclonal anti-Rho antibody. AGE-BSA increased Rho-GTP level. (B) HUVECs were treated with or without 50 μg/ml AGE-BSA for 10 min. Lysates were immunoprecipitated with anti-RAGE monoclonal antibody (a), or anti-RhoA monoclonal antibody (b). Immunoprecipitates were subjected to Western blot analysis using anti-RAGE and anti-Rho monoclonal antibodies to confirm adequate immunoprecipitation. Representative results of five experiments performed with similar results.

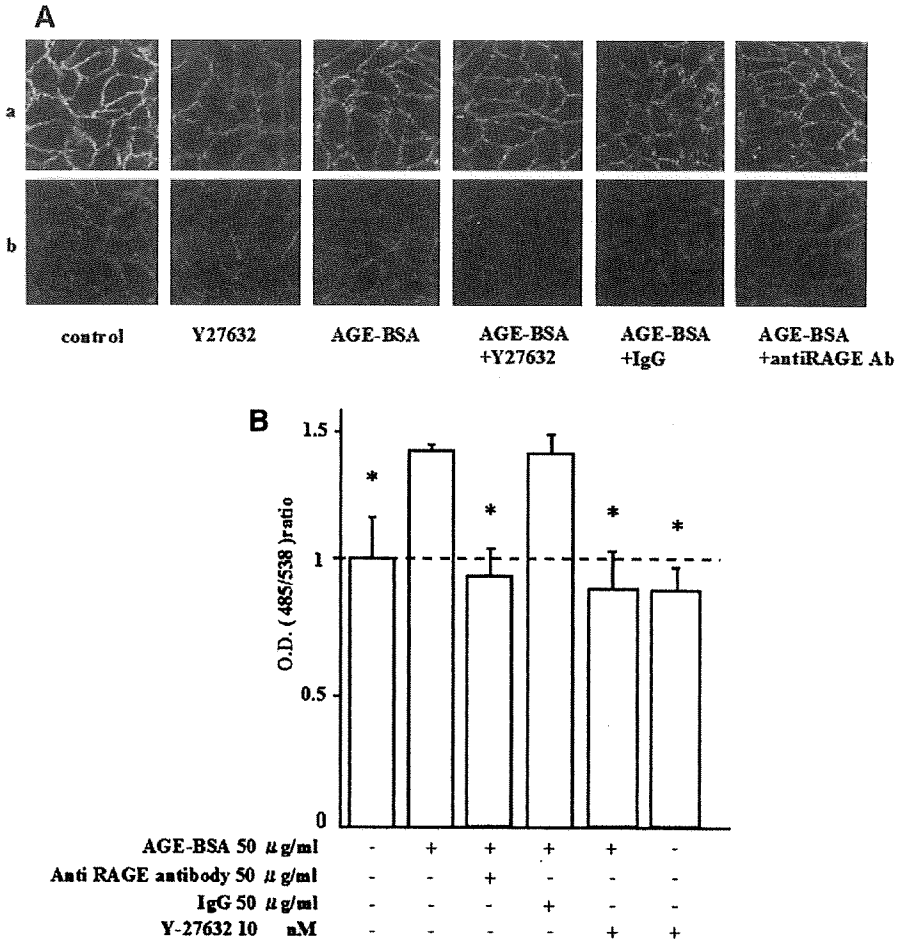

Fig. 4. Rho/Rho kinase inhibitor and anti-RAGE antibody blocked AGE-BSA-induced gap formation with actin reorganization and transendothelial hyperpermeability. (A) HUVECs grown on fibronectin-coated glass-bottom dishes were pretreated with Y27632 (10 μM) then exposed to 50 μg/ml AGE-BSA for 6 h. After incubation, cells were fixed and processed for immunofluorescence analysis of VE-cadherin and actin. Rho kinase inhibitor decreased gap formation and actin reorganization induced by AGE-BSA. (B) HUVEC on Transwell inserts were pretreated with Y27632 (10 μM) or anti-RAGE antibody (50 μg/ml), then exposed to 50 μg/ml AGE-BSA for 6 h. After incubation, FITC-labeled dextran was added and transendothelial diffusion of dextran was calculated. Rho kinase inhibitor and anti-RAGE antibody decreased permeability induced by AGE-BSA. Data are expressed as means ± S.D. ($n = 3$). $^*P < 0.05$, compared with the group treated with 50 μg/ml AGE-BSA alone.

functions [13]. Our study showed that AGEs activates RhoA in endothelial cells, leading to increased hyperpermeability through actin polymerization.

RAGE is a member of the immunoglobulin superfamily of receptors [14]. Receptor for IL-1β is also one of the immunoglobulin superfamily of receptors and the Rho family is a component of the IL-1 receptor complex [15]. In our study, RAGE and RhoA also formed a complex with or without stimulation with AGE. Because RhoA and RAGE spontaneously form a complex, it is likely that AGE directly activates RhoA. However, further studies including animal experiments are necessary to clarify the mechanism of RhoA activation by AGE-BSA.

In summary, our results demonstrated that AGE-BSA induces reorganization of the actin cytoskeleton through RAGE/Rho activation, leading to endothelial cell hyperpermeability.

Acknowledgments

This work was supported in part by a Grant-in-Aid for Scientific Research by the Ministry of Health, Labor and Welfare of Japan, the Ministry of Education, Culture, Sports, Science and Technology of Japan and University of Occupational and Health, Japan.

References

[1] Viberti, G.C. (1983) Increased capillary permeability in diabetes mellitus and its relationship to microvascular angiopathy. Am. J. Med. 75, 81–84.
[2] Esposito, C., Gerlagh, H., Brett, J., Stern, D. and Vlassara, H. (1989) Endothelial receptor-mediated binding of glucose-modified albumin is associated with increased monolayer permeability and modulation of cell surface coagulant properties. J. Exp. Med. 170, 1387–1407.
[3] Otero, K., Martínez, F., Beltrán, A., González, D., Herrera, B., Quintero, G., Delgado, R. and Rojas, A. (2001) Albumin-derived advanced glycation end-products trigger the disruption of the vascular endothelial cadherin complex in cultured human and murine endothelial cells. Biochem. J. 359, 567–574.
[4] Guo, X.H., Huang, Q.B., Chen, B., Wang, S.Y., Li, Q., Zhu, Y.J., Hou, F.F., Fu, N., Brunk, U.T. and Zhao, M. (2006) Advanced glycation end products induce actin rearrangement and subsequent hyperpermeability of endothelial cells. APMIS 114, 874–883.
[5] Yuan, S.Y. (2000) Signal transduction pathways in enhanced microvascular permeability. Microcirculation 7, 395–403.
[6] Antonetti, D.A., Lieth, E., Barber, A.J. and Gardner, T.W. (1999) Molecular mechanisms of vascular permeability in diabetic retinopathy. Semin. Ophthalmol. 14, 240–248.
[7] Salameh, A., Zinn, M. and Dhein, S. (1997) High D-glucose induces alterations of endothelial cell structure in a cell-culture model. J. Cardiovasc. Pharmacol. 30, 182–190.
[8] Yu, P.K., Yu, D.Y., Cringle, S.J. and Su, E.N. (2005) Endothelial F-actin cytoskeleton in the retinal vasculature of normal and diabetic rats. Curr. Eye Res. 30, 279–290.

[9] Makita, Z., Radoff, S., Rayfield, E.J., Yang, Z., Skolnik, E., Delaney, V., Friedman, E.A., Cerami, A. and Vlassara, H. (1991) Advanced glycosylation end products in patients with diabetic nephropathy. New Engl. J. Med. 325, 836–842.
[10] Goldin, A., Beckman, J.A., Schmidt, A.M. and Creager, M.A. (2006) Advanced glycation end products: sparking the development of diabetic vascular injury. Circulation 114, 597–605.
[11] Tanikawa, R., Tanikawa, T., Okada, Y., Nakano, K., Hirashima, M., Yamauchi, A., Hosokawa, R. and Tanaka, Y. (2008) Interaction of galection-9 with lipid rafts induces osteoblast proliferation through the c-Src/ERK signaling pathway. JBMR 23, 278–286.
[12] Huttunen, H.J., Fages, C. and Rauvala, H. (1999) Receptor for advanced glycation end products (RAGE)-mediated neurite outgrowth and activation of NF-κB require the cytoplasmic domain of receptor but different downstream signaling pathways. J. Biol. Chem. 274, 19919–19924.
[13] Riento, K. and Ridley, A.J. (2003) Rocks: multifunctional kinases in cell behaviour. Nat. Rev. Mol. Cell Biol. 4, 446–456.
[14] Neeper, M., Schmidt, A.M., Brett, J., Yan, S.D., Wang, F., Pan, Y.C., Elliston, K., Stern, D. and Shaw, A. (1992) Cloning and expression of a cell surface receptor for advanced glycosylation end products of proteins. J. Biol. Chem. 267, 14998–15004.
[15] Singh, R., Wang, B., Shirvaikar, A., Khan, S., Kamat, S., Schelling, J.R., Konieczkowski, M. and Sedor, J.R. (1999) The IL-1 receptor and Rho directly associate to drive cell activation in inflammation. J. Clin. Invest. 103, 1561–1570.